CHEMISTRY
A EUROPEAN JOURNAL

DOI: 10.1002/chem.200800444

Extended Surface Chirality for Enantiospecific Adsorption

Pawel Szabelski*[a]

Abstract: A rapid development of nanotechnology opens up a way for the fabrication of solid surfaces containing unique adsorption properties. In this article, we present the concept of a chiral nanostructured surface as a potential environment for the separation of chiral molecules. In particular, we focus on the effect of size and shape of the adsorbing molecules on the effectiveness of their separation on a surface with a special distribution of active sites. The Monte Carlo simulation method was used to study enantiospecific adsorption of model chiral molecules that differ in molecular footprint and adsorption energy. It was demonstrated that manipulating the footprint offers many possibilities for tuning the preference of the surface for adsorption of a selected enantiomer. One interesting finding was that subtle differences in the interaction pattern of the molecule with the chiral surface can lead to a reversal of enantioselectivity. The results of this work highlight the role of extended surface chirality in enantiospecific adsorption of enantiomers. They also suggest that the proposed mechanism of chiral selection can be a realistic alternative to those inherent in conventional enantioselective adsorbents.

Keywords: adsorption · chirality · computer chemistry · nanostructures · surface chemistry

Introduction

Separation of enantiomers is a challenging task in the production of enantiopure chemicals. This is particularly true for pharmaceutical, agrochemical and food industries, the products of which are digested by living organisms. It has long been known that while one enantiomer can have a desired (e.g. therapeutic) effect, the other can be neutral or even toxic. Thus, because most new drugs are marketed as single enantiomers, special care should be taken to produce chiral pharmaceuticals of extremely high purity.[1] One way to achieve this goal is to separate the preferred therapeutic enantiomer from a racemate. Liquid chromatography, which uses chiral stationary phases (CSPs), holds a leading position in this field.[2,3] The CSPs used in chiral chromatography usually consist of an achiral matrix (e.g. porous silica) with bonded chiral ligands. Among them the most prevalent are small groups (e.g. Pirkle phases[4]) or macromolecules including cellulose derivatives[5–9] and proteins.[10,11] Despite the different physicochemical properties of various CSPs, enantioselective adsorption processes carried out in their presence are controlled by the same or very similar mechanisms. Namely, the adsorption on CSPs is usually considered to take place on two kinds of sites that are common for all types of stationary phases mentioned above. The first type refers to chiral selectors (chiral ligands) that are responsible for the selective differentiation between the components of the racemic mixture, whereas the second embraces the "background" nonselective sites (achiral matrix).

Note that, although CSPs are the most popular enantioselective adsorbents, they are not the only materials of this kind which have been synthesised so far. A rapid development of methods to fabricate chemically and structurally modified surfaces to exhibit global or local chirality has brought new possibilities for enantioseparations.[12–18] Recently, there has been a growing interest in chiral surfaces that are created by using single crystal planes. Two of the most promising candidates in this field are naturally chiral surfaces[19–24] and metallic surfaces templated with organic modifiers.[16–18,25–29] Naturally chiral surfaces are usually obtained by cleavage of achiral bulk metallic structures[19–24] or exposure of the surfaces of naturally chiral crystals.[30,31] The resulting surface has a unique structure, for example, a unique arrangement of kinks and steps, which is not superimposable on its mirror image and is thus chiral. Because of the chirality, the surface interacts more strongly with those molecules that are complementary to the surface, that is,

[a] Dr. P. Szabelski
Department of Theoretical Chemistry
Maria Curie-Sklodowska University
Pl. M. C. Sklodowskiej 3, 20031 Lublin (Poland)
Fax: (+48) 081-537-5620
E-mail: szabla@vega.umcs.lublin.pl

they fit chiral nanostructures. It has been shown both experimentally[22,23,25–29] and theoretically[22,32–34] that naturally chiral surfaces have a clear preference for adsorption of the complementary enantiomer. A similar effect has also been observed in the case of metallic crystal faces templated with modifiers, such as tartaric acid,[35] cinchona alkaloids,[12] or 2-butanol.[25,28] In those instances the origin of enantioselection is, however, greatly debated and is attributed to, for example, direct modifier–substrate interactions on the metal surface, the stability of diastereomeric complexes of the substrate and the modifier or adsorbate-induced restructuring of metal single-crystal surfaces.[36]

A general picture emerging from the experimental studies of adsorption on chiral surfaces shows that this process is rather complex, because it is affected by many factors, which are often difficult to control precisely under experimental conditions. These include, for example, the above-mentioned adsorbate-induced surface reconstruction[36] or thermally driven fluctuations in surface geometry.[37] For this reason, substantial theoretical efforts have been made to understand the origins of enantioselectivity of chiral nanostructures. For example, mechanisms of binding of chiral analytes to various CSPs have been extensively studied by using molecular dynamics docking simulations[38–42] and the Monte Carlo (MC) method.[38,39,43] In the case of naturally chiral surfaces, MC simulations have been performed by Sholl and co-workers to study adsorption of chiral hydrocarbons[33–35] on stepped platinum surfaces. Recently, plane-wave DFT has also been used to examine adsorption of small chiral amino acids on copper[36] and gold.[22] With regard to chirally templated surfaces, the adsorption of chiral molecules has been modelled theoretically by using statistical mechanics and the MC method.[44–47] A direct observation from the studies cited above is that the enantioselectivity of chiral surfaces originates mainly from specific intermolecular interactions between a well-defined chiral centre and the complementary enantiomer. In this case, a one-to-one correspondence is usually preserved such that the local chirality of the surface is the deciding factor in the enantiodiscrimination process.

Recently, we have started systematic investigations of a model chiral surface that provides a new mechanism of selective differentiation between enantiomers.[48–52] We demonstrated that the one-to-one correspondence that is common for most of the chiral adsorbents described briefly in this section is not a necessary condition for the selective adsorption of a selected enantiomer. The proposed approach was based on the difference between molecular footprints of enantiomers adsorbing on a solid surface with a special distribution of active sites. In previous work we considered adsorption of short-chain rigid molecules composed of four identical segments, representing that part of a bulk chiral molecule that directly contacts the surface.[48–52] The obtained results indicated clearly that the preference of the surface for adsorption of one enantiomer can be easily tuned by manipulating energetic properties of the surface. The main purpose of this study is to examine further possibilities for tuning the selectivity by changing the size, shape and chemical composition of the chiral molecules. The model described here was meant to be quite general with no relation to any specific experimental system. Instead, our objective was to identify the factors that affect the separation of enantiomers and to provide some hints at how to correlate the structure of the surface with the geometry of the adsorbate. To this end we used the MC simulation method and provided simple analytical solutions of our model.

Computational Methods

We consider the adsorption of model chiral molecules on a solid surface to be represented by a square lattice of binding sites with well-defined binding energies. The chiral molecules are modelled as rigid chain structures composed of a different number of segments. A molecular segment can be an atom or a functional group occupying one binding site. In the simplified approach adopted here, only that part of the molecule which directly contacts the surface is considered. The remaining parts of the molecule that are not involved in the adsorption are disregarded and assumed to be responsible only for preservation of chirality in the bulk phase. According to this assumption, the only important structural property of the molecule is the footprint it leaves on the surface. Figure 1 shows the simplest example of chiral footprints consisting of four adsorption sites, each occupied by one segment of the adsorbed enantiomer. These footprints correspond to the adsorption of the enantiomers of the Γ-shaped molecule, which we call the original molecule **Γ**. The original molecule is assumed to consist of four identical segments, as shown in the centre of the top frame in Figure 2.

To examine the effect of the footprint shape, we modified the structure of the original molecule by adding one segment. For the sake of generality, we assumed that the additional segment can have different chemical properties from the segments of the original molecule. Figure 2 shows schematically the molecular structures obtained by the addition of the segment. These planar molecules are called homogeneous or heterogeneous, depending on whether the additional segment is the same as the four remaining segments or not, respectively. As seen in Figure 2, the resulting molecules can be divided into two groups: those that retain chirality when the chain composition is homogeneous (**A**–**F**) and those that lose chirality (**X**–**Z**) under these circumstances.

The adsorbing surface used in our model consisted of two types of sites the strengths of interaction of which with a single segment of a molecule were markedly different. In particular, for homogeneous molecules the energy of interaction between an active site and a segment of the molecule was characterised by ε_a, whereas that between an inert site and the segment by ε_b. To construct a surface selective towards one of the enantiomers, the active sites were distributed on a square lattice in such a way that the chosen enantiomer could adsorb more strongly than the other, as assumed in our previous work.[48–52] An example of the distribution meeting this requirement is shown in the top part of Figure 1 for the *S*-selective surface. This distribution has been used successfully to separate the enantiomers of the original Γ-shaped molecule.[50]

We will now indicate possible connections of the model chiral surface with some real cases. The surface shown in Figure 1 can be treated as, for example an exposed (100) fcc (face-centred cubic) face of a hypothetical binary alloy crystal with a somewhat unusual arrangement of atoms. However, it is worth noting that the active sites in Figure 1 form an ordered $(\sqrt{5}\times\sqrt{5})R27^{\circ}$ superstructure that has been observed experimentally for various adsorption systems including, for example, oxygen atoms on Mo(001)[53] and Pd(100)[54] or Yb atoms on Al(001).[55,56] Recently, homochiral nanoporous 2D arrays in which nanocavities form an ordered pattern resembling that in Figure 1 have also been reported.[57] These chiral supramolecular structures have been obtained by hierarchical as-

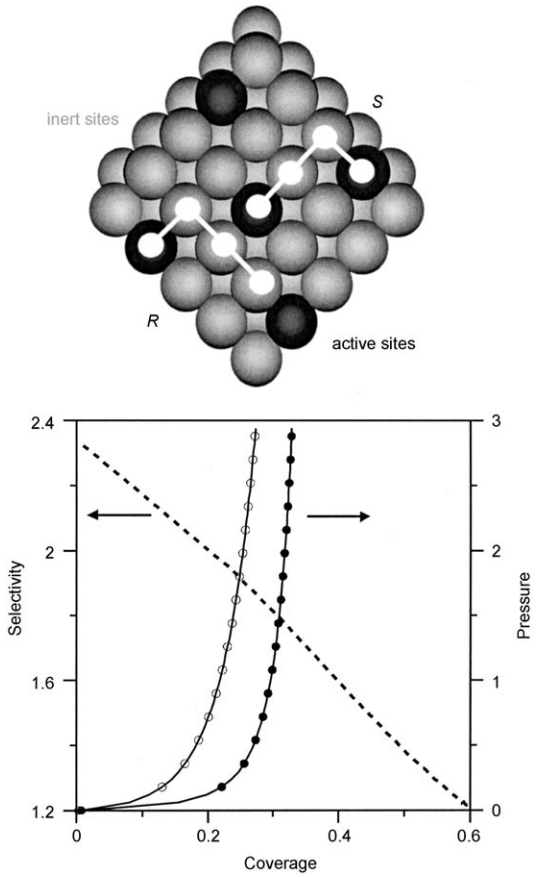

Figure 1. Schematic view of the unit cell of the nanostructured chiral surface (top). The thick lines represent the simplest non-superimposable footprints of a chiral molecule occupying four adsorption sites. The adsorbed configuration shown in the top part illustrates the difference in the maximum number of the active sites that are accessible to enantiomers *R* (one active site) and *S* (two active sites). The unit cell from the top part corresponds to the *S*-selective surface. The bottom part shows partial adsorption isotherms (——); ○: *R* enantiomer, ●: *S* enantiomer and the selectivity (-----) calculated for the racemic mixture of the *R* and *S* enantiomers adsorbed on the *S*-selective surface. Pressure is given in arbitrary units.

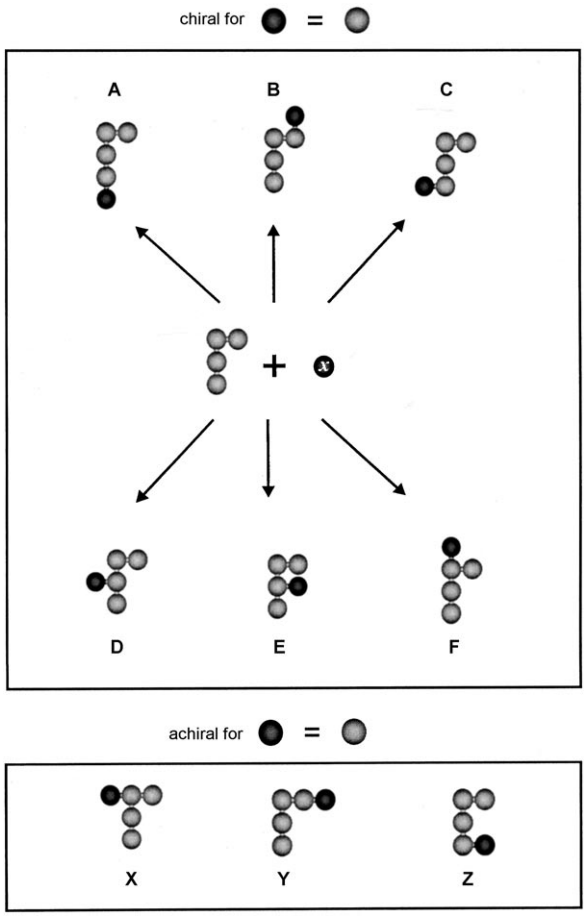

Figure 2. Method of construction of the chiral molecules used in the simulation. The molecules shown in the figure are the possible products of addition of a single molecular segment, **X**, to the original Γ-shaped molecule shown in the centre of the top frame. These adducts are called *S* enantiomers. The three molecules from the bottom frame lose chirality when the energy of interaction between the additional segment and the chiral surface is the same as for the remaining part of the molecule.

sembly of organic molecules. The experimental results mentioned above suggest that the structure presented in Figure 1 can be viewed as a prototype of a chiral surface the active sites of which can be created in many different ways. For example, the active sites can be guest atoms, crystal vacancies, nanocavities or nanoscopic molecular domains created on solid surfaces.[58] In this context, the proposed model should be applicable to a wide range of systems involving adsorption on chiral nanostructured substrates.

We consider adsorption of racemic, that is, equimolar mixtures of the enantiomers of molecules **A**–**Z**. The adsorption of the enantiomers was assumed to be submonolayer with no lateral interactions in the adsorbed phase. Moreover, no surface diffusion of the adsorbed molecules was allowed.[49] Molecules **A**–**Z** were assumed to adsorb exclusively in a planar configuration, contacting the surface with all five segments. The MC simulations were carried out on a 2D, $L \times L$ lattice of adsorption sites with $L = 50$. Accordingly, the resulting surface consisted of 10×10 unit cells shown in the top part of Figure 1. We used the simulation method developed for equilibrium adsorption of polyatomics on solid surfaces. Specifically, the simulations were performed by using a standard grand canonical MC technique for localised adsorption of *k*-mers on a square lattice.[59–61] This simulation technique was described in detail in our earlier work.[48–50,52]

In this study we use two simple functions that are useful to describe the mixed adsorption. These are: the surface coverage and the selectivity. The surface coverage is defined as the ratio of the number of adsorption sites occupied by the molecules of a given type/handedness to the total number of adsorption sites on the surface, L^2. The surface coverage plotted against pressure gives an equilibrium adsorption isotherm of a selected species. We note that the adsorption isotherms described in this study always refer to the coverage expressed as a function of the total pressure of the racemate. The selectivity in our model is obtained by dividing the surface coverage of an *S* enantiomer by the surface coverage of an *R* enantiomer. Additionally, we introduce the selectivity at the zero-pressure limit, E_o, which carries information about the adsorption of the enantiomers under very low pressures and thus under very low coverages.

The coverage of each enantiomer at a fixed pressure was an average of over 50 to 100 independent MC runs. For each value of pressure, up to 40000 MC steps, in which one MC step is defined as L^2 attempts of changing the system state, were performed to reach equilibrium. In the case of the selectivity at the zero-pressure limit, the corresponding values were obtained by assuming a pressure varying between 10^{-12} and 10^{-6}. For the sake of generality, in the following we express all of the energies in kT units and use dimensionless units of pressure. Most of the results

discussed in this work refer to $\varepsilon_a = 2.0$ and $\varepsilon_b = 0.0$ unless otherwise indicated.

Results and Discussion

To examine the effect of the footprint shape we carried out MC simulations of the adsorption of the modified molecules from Figure 2. For comparative purposes, in the bottom part of Figure 1 we show the partial isotherms of the *R* and *S* enantiomers of the original Γ-shaped molecule adsorbed on the *S*-selective surface. These results were obtained for $\varepsilon_a = 2.0$ and $\varepsilon_b = 0.0$ and they correspond to the reference adsorption system in our investigations. Before we proceed with the modified molecules let us focus on the curves plotted in Figure 1. As seen in this figure, the simple pattern of active sites shown in Figure 1 (top) provides preferential adsorption of the *S* enantiomer, regardless of pressure/coverage. Specifically, the isotherm of the *S* enantiomer always runs above that of the *R* enantiomer, which results in a selectivity at the zero-pressure limit equal to 2.33. Another important effect is that the selectivity (-----) decreases in a nearly linear fashion with coverage. The main objective of the following discussion is to demonstrate how the modification of the original molecule influences the dependencies shown in Figure 1.

Homogeneous molecules: Figure 3 shows the partial adsorption isotherms of the enantiomers of the homogenous molecules from the top frame of Figure 2. The results plotted in the figure were simulated for the corresponding racemic mixtures adsorbed on the *S*-selective surface. As can be seen in Figure 3, the footprint shape has a profound effect on the behaviour of the partial adsorption isotherms. This refers primarily to the relative position of the isotherms calculated for enantiomers *R* and *S* of the same chiral molecule. The overall shape of the isotherms is, in general, weakly sensitive to the changes in the footprint geometry. Figure 3 clearly shows that there are two different ways in which the enantiomers adsorb on the *S*-selective surface, depending on their shape. Namely, for molecules **A** and **D** we observed that the distance between the isotherms for the *R* and *S* enantiomers is very small, especially at low pressures. This effect means no clear preference of the *S*-selective surface for adsorption of the *S* enantiomer. One interesting finding is that for molecule **D** the selectivity of the adsorbing surface is reversed at elevated pressures. In this case, the *R* enantiomer of molecule **D** (-----) adsorbs somewhat more strongly relative to the *S* enantiomer (——), as seen in the isotherm graph for **D**. Nevertheless, the advantage of an *R* over an *S* configuration is minimal and results in a selectivity varying from 0.96 to 1.00. On the contrary, for molecules **B**, **C**, **E** and **F** we observed that the *S*-selective surface exhibits enhanced selectivity for the complementary enantiomer. An extreme example is molecule **C**, for which the gap between the partial adsorption isotherms of the *S* and *R* enantiomer is the largest among the results shown in Figure 3.

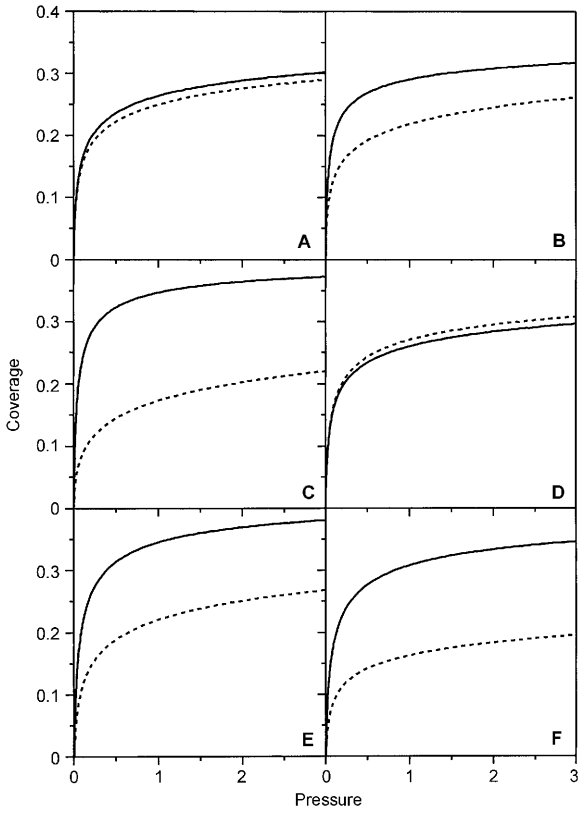

Figure 3. Partial isotherms of adsorption of the enantiomers of molecules **A**–**F** on the *S*-selective surface (——: *S* enantiomers, -----: *R* enantiomers). The results plotted in the figure correspond to the molecules composed of five identical segments. Pressure is given in arbitrary units.

The unusually high selectivity towards the *S* enantiomer of molecule **C** originates partially from the fact that the opposite enantiomer of this molecule cannot occupy two active sites when adsorbed on the *S*-selective surface. This can be easily imagined by visualising the enantiomers of molecule **C** adsorbed within the unit cell shown in Figure 1. A similar observation refers also to molecules **E** and **F**. On the other hand, the opposite situation takes place in the case of molecules **A** and **D** the *R* and *S* enantiomers of which are both able to occupy two active sites on the *S*-selective surface. This suggests that the possibility of the *R* and *S* enantiomers occupying two active sites is the key factor that reduces the selectivity, especially at low coverages. Note, however, that molecule **B** is a significant departure from this rule. Here, although both enantiomers of molecule **B** can occupy two active sites, the distance between the partial isotherms shown for **B** is quite large. Explanation of the differences observed in adsorption of molecules **A**–**F** requires a closer inspection of the possible configurations of each enantiomer on the *S*-selective surface. We will come back to this problem later in this section.

To better highlight the differences in the adsorption of the chiral molecules from Figure 2, let us examine more closely the dependence of the selectivity on the surface coverage. Figure 4 shows the selectivity as a function of the total sur-

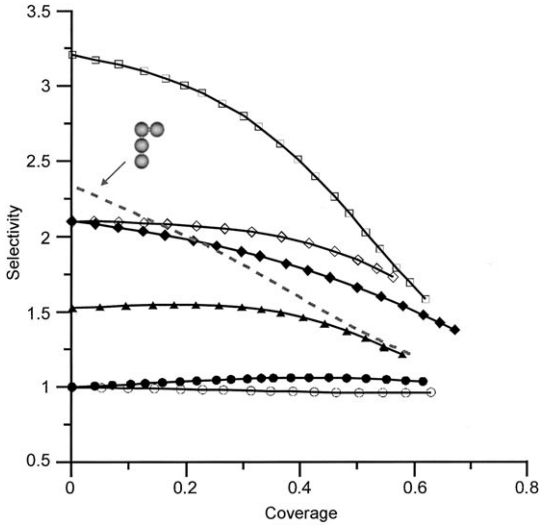

Figure 4. Influence of the surface coverage on the selectivity calculated for the molecules from Figure 2. The curves plotted in the figure were obtained for the adsorption of the corresponding racemates on the *S*-selective surface. The selectivity curves of the molecules are represented as follows: ●: **A**; ▲: **B**; □: **C**; ○: **D**; ◆: **E**; ◇: **F**. The grey dashed line shows the selectivity calculated for the original Γ-shaped molecule.

face coverage simulated for molecules **A**–**F**. For comparative purposes, we also plotted the selectivity curve corresponding to the original Γ-shaped molecule (-----). The most important information from Figure 4 is the relative position of curves **A**–**F** and their position with respect to the curve obtained for the original Γ-shaped molecule. We can observe that for coverages lower than about 0.05, the selectivity decreases in the order $\mathbf{C} > \mathbf{\Gamma} > \mathbf{E},\mathbf{F} > \mathbf{B} > \mathbf{A}$, **D**. This indicates clearly that the structural modification of the original molecule is beneficial for the separation only when the product is molecule **C**. Moreover, an additional advantage of molecule **C** is that the improvement in the selectivity applies to the entire coverage range. The opposite effect takes place in the case of molecules **A** and **D** for which the selectivity is substantially lower than for molecule **Γ**, regardless of coverage. In the case of molecule **B**, we are dealing with a somewhat different situation. Specifically, the selectivity obtained for **B** is initially considerably lower than for **Γ**, but with increasing coverage it becomes very close to that calculated for the original molecule. Finally, for molecules **E** and **F** a combination of the two trends described above can be seen. In these cases, the structural modification of molecule **Γ** leads to an improvement in the selectivity only at sufficiently high surface coverages. That is, the selectivity simulated for molecules **E** and **F** is lower than for molecule **Γ** as long as the coverage does not exceed 0.25 and 0.15, respectively. An interesting observation is that the selectivities corresponding to molecules **E** and **F** approach the same value 2.10 as the coverage tends to zero.

One more valuable piece of information from Figure 4 is how the structural modification of molecule **Γ** affects the shape of the selectivity curves. Contrary to the case with molecule **Γ**, the selectivity curves calculated for the modified molecules are strongly non-linear. Moreover, their slopes are markedly different. For most of the chiral molecules the selectivity decreases appreciably with coverage. As seen in Figure 4, the onset of the decrease in selectivity is strongly influenced by the footprint shape. In the case of molecule **C,** the selectivity drops sharply and continuously with increasing coverage, especially when the coverage is sufficiently high. For the remaining curves we can observe much less rapid changes. For example, the selectivity simulated for molecules **B** and **F** remains nearly constant up to a coverage equal to 0.3. This shows that the chiral surface retains the initial selectivity for the *S* enantiomer of either **B** or **F** within a relatively wide interval of coverages. Interestingly, for molecules **A** and **B** a weak increasing trend in the selectivity can be observed at low and moderate coverages. Note, however, that the increases in selectivity associated with molecules **A** and **B** are negligible relative to the changes observed for the remaining molecules, especially for molecule **C**.

The differences in adsorption of molecules **A**–**F** that are observed at high surface coverages originate mainly from different packing geometries of the enantiomers of these molecules. In this case, interaction of the enantiomers with the surface is largely influenced by steric exclusion. For example, nanocavities formed in the mixed adsorbed layer by surrounding molecules can be of the shape of the preferred enantiomer *S* or they can accommodate only the opposite enantiomer. In the latter case, the surface can lose the preference for adsorption of the complementary enantiomer as the coverage increases, which in extreme cases can lead to reversal of selectivity. Evidently, this effect is strongly dependent on the footprint shape, resulting in a case-sensitive behaviour of the selectivity at high coverages. On the contrary, the common decreasing trend in selectivity that was observed for most of the chiral molecules from Figure 4 has a simpler explanation. In this case, the dominating factor that reduces the selectivity is competition between the enantiomers for occupation of the active sites. Specifically, when the coverage increases, the surface loses it preference for adsorption of *S* enantiomers because the clusters of active sites matching the footprint of enantiomer *S* (clusters with two active sites) are partially occupied by the opposite enantiomer. This general tendency involving blockage of chiral centres has also been observed for adsorption of racemic mixtures on other chiral adsorbents, such as CSPs[47,62] and chirally templated surfaces.[46] A combination of the two effects described above results in a largely diversified interaction pattern of the enantiomers with the chiral surface. This makes theoretical description of the selectivity at high coverages quite difficult. A much simpler situation arises when dealing with an extremely low density of the adsorbed phase. Under these conditions the competition in occupation of the active sites is practically eliminated such that the enantiomers are able to adopt energetically preferred configurations. In this case, the selectivity is dictated mainly by the difference between the adsorption energies associated with

the *R* and *S* enantiomers and thus it can be easily calculated.

The influence of the footprint shape on the selectivity at low adsorbate densities can be predicted by using simple thermodynamic considerations. Specifically, to predict the selectivity for any of the molecules **A**–**F** it is sufficient to determine Henry's constants for the corresponding enantiomers, *R* and *S*. Then, the selectivity at the zero-pressure limit, E_o, is defined as a ratio of the Henry's constants (*S* enantiomer/*R* enantiomer). The Henry's constants can be obtained by identifying possible configurations of an adsorbed enantiomer within the unit cell from Figure 1 and enumerating those configurations that have the same adsorption energy. Note that in our case this task is particularly easy because for each of the homogeneous molecules shown in Figure 2 there are only three possible values of the adsorption energy. They correspond to the number of active sites occupied by a given enantiomer and are equal to: $2\varepsilon_a+3\varepsilon_b$ (two active sites), $\varepsilon_a+4\varepsilon_b$ (one active site) and $5\varepsilon_b$ (no active sites). The enumerating procedure gives the adsorption energy distribution (AED) that carries sufficient information to calculate the Henry's constants. A detailed description of the method outlined briefly above can be found in our previous work.[48–52]

Table 1 shows the selectivity at the zero-pressure limit calculated for the homogeneous molecules **A**–**Z**. In the second column of the table we listed the expressions that allow for the calculation of the selectivity corresponding to a given footprint shape. These results show clearly that the surface is intrinsically achiral for molecules **A** and **D**, as seen in Figure 4. Note also that in the remaining cases the selectivity is a simple function of the difference between the adsorption energies associated with the active and inert site, $\Delta\varepsilon$. This useful property makes tuning of the selectivity easier because only one of the adsorption energies has to be changed while the other can be held constant. In real situations this would require, for example, changing the adsorptive properties of the active sites by replacement of one atom or cavity type by another. The third column of Table 1 shows the selectivity calculated by means of the expressions from the second column, for the same set of parameters as that used in Figure 4 ($\varepsilon_a=2.0$ and $\varepsilon_b=0.0$). The values predicted theoretically agree perfectly with the MC results from Figure 4. The last column of Table 1 shows the upper limit of the selectivity at the zero-pressure limit, calculated for different molecular footprints. As can be seen in the table, the selectivity shows three different types of limiting behaviour. Specifically, for molecules **A** and **D** increasing the energy gap between the active and inert sites does not lead to any improvement in the selectivity. On the contrary, for molecules **C**, **E** and **F** the selectivity can be theoretically increased up to infinity. The third possibility is that the selectivity tends to 2, as seen for molecule **B**.

Table 1. Selectivity at the zero-pressure limit, E_o, obtained from the theory for the chiral molecules composed of one type of segment.

Molecule	E_o[a]	E_o ($\Delta\varepsilon=2.0$)	E_o^{∞}[b]
A, **D**, **X**, **Y**, **Z**	1	1.00	1.00
B	$(2\varphi-1)/(\varphi+1)$	1.52	2.00
C	$0.2(2\varphi-1)$	3.21	unlimited
E, **F**	$0.2(\varphi+1)$	2.10	unlimited

[a] $\varphi=2[\cosh(\Delta\varepsilon)+1]$. [b] $|\Delta\varepsilon|\rightarrow\infty$.

Summarising the key findings of this section, we can conclude that of the six homogenous molecules depicted in Figure 2, the enantiomers of only **C**, **E** and **F** are better separated with the chiral surface, relative to the original molecule **Γ**. However, the improvement in the selectivity observed in the case of molecules **E** and **F** occurs only within a limited interval of coverages, that is, at sufficiently high densities of the adsorbed phase. The main advantage of molecules **C**, **E** and **F** is the possibility of improving the selectivity by, for example, increasing the adsorption energy of a single molecular segment on the active site. Note that for these molecules the selectivity can be increased also in the opposite way, by decreasing the energy of adsorption of a single segment on the inert site. In this case, an interesting possibility opens up for manipulating the selectivity.

Effect of the energetic landscape of the surface: As seen in Table 1, the selectivity at the zero-pressure limit depends only on the energy gap between the active and inert sites. A closer inspection of the expressions listed in the second column of Table 1 reveals that the selectivity is an even function of the energy gap. This property provides new opportunities for tuning the selectivity. In particular, for molecules **B**, **C**, **E** and **F** it is possible to interchange the active sites with the inert sites to obtain the same selectivity as for the original surface. Specifically, to maintain constant selectivity the energies of adsorption ε_a and ε_b can be changed arbitrarily, but in such a way that the absolute value of the difference between them remains constant. To demonstrate this in Figure 5 we plotted the selectivity as a function of the energy gap, assuming that $\varepsilon_a=2.0$ and that ε_b varies between -6.0 and 6.0. The top part of this figure illustrates schematically the interchange of adsorption sites a and b. As can be seen in Figure 5, for molecules **B**, **C**, **E** and **F** the assumed change in the adsorption energies does not induce any change in the selectivity. For example, in the case of molecule **C** it is possible to construct two chiral surfaces that are characterised by the selectivity at the zero-pressure limit equal to 3.21 (see Table 1). One of them is the surface with $\varepsilon_a=2.0$ and $\varepsilon_b=0.0$, whereas for the other surface the energy parameters are $\varepsilon_a=2.0$ and $\varepsilon_b=4.0$. A similar argument applies to the remaining molecules from Figure 2, except for the original Γ-shaped molecule. The selectivity for molecule **Γ** is represented by the thick grey line in Figure 5. It was calculated by using the expression derived in our previous work.[48–52] One striking property of the results obtained for the Γ-shaped molecule is that the corresponding selectivity curve is not symmetrical with respect to the dashed vertical line plotted at $\Delta\varepsilon=0$. The selectivity approaches the limiting value 2 as the energy gap becomes suf-

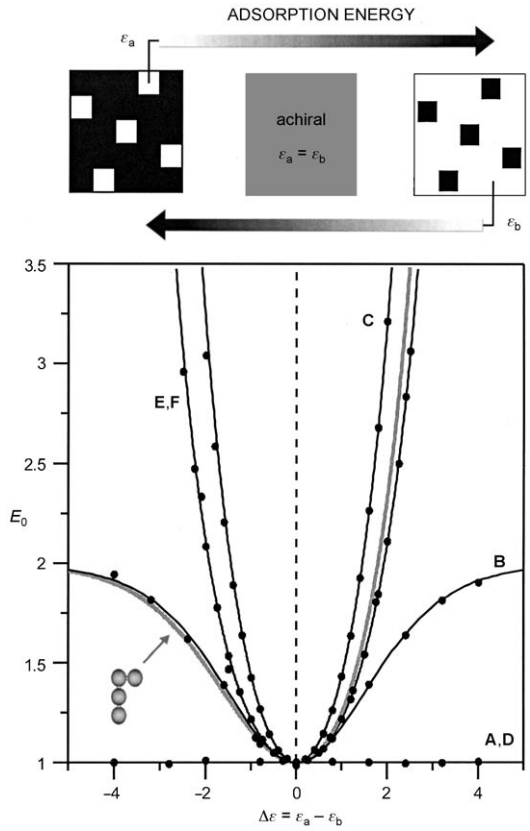

Figure 5. Effect of the energetic properties of the chiral surface on the selectivity at the zero-pressure limit calculated for the molecules from Figure 2. The symbols are the results of the MC simulations, whereas the lines are the predictions of the theory. The grey solid line shows the selectivity calculated for the original Γ-shaped molecule. The scheme in the top part illustrates how the energetic properties of the surface can be tuned by changing the energy of adsorption of a single segment on the active (ε_a) and inert site (ε_b). A darker shade of grey in the energy bar means a stronger interaction between the segment and the site.

ficiently negative, but it is unlimited for positive values of the energy gap. Moreover, for negative values of the energy gap the selectivity curve obtained for **Γ** is nearly identical to that calculated for molecule **B**. The above effects show that the altered molecular structures **B**, **C**, **E** and **F** are, in general, better candidates for the chiral separation than the original Γ-shaped molecule. The reason for this is twofold. Firstly for molecules **B**, **C**, **E** and **F** the change in the energetic landscape of the surface does not lead to a deterioration of the selectivity. This advantage can be used, for example, when the fabrication of the chiral surface with $\varepsilon_a > \varepsilon_b$ is not possible for some technical reasons. In this case, the enantiomers of these four molecules can be separated on the surface with the opposite energetic landscape and the effectiveness of the separation would be the same as for the original surface. Secondly, the change of the molecular shape from form **Γ** to **E** or **F** results in a significant improvement in the selectivity when the separation occurs on the surface with the opposite energetic landscape (see the left part of Figure 5).

Heterogeneous molecules: Let us now present one more interesting possibility for tuning the selectivity. Here, in addition to the structural changes shown in Figure 2, we assume that molecules **A**–**Z** have non-uniform chemical composition. For this purpose, we assume that the additional segment **X** has markedly different chemical properties from the remaining part of the molecule. This assumption results in the three new chiral structures that are shown in the bottom frame of Figure 2. The energy of adsorption of segment **X** on the active site was characterised by ε_x. For the sake of simplicity we assumed that the energy of adsorption of this segment on the inert site was set equal to zero, as for the four remaining segments. Figure 6 shows the selectivity at the zero pressure limit as a function of the adsorption energy of the additional segment calculated for $\varepsilon_a = 2.0$. The dashed vertical line corresponds to the homogeneous composition of the chiral molecules, that is, to $\varepsilon_x = \varepsilon_a$. As can be seen in Figure 6, changing the adsorption energy of the additional segment provides wide possibilities for tuning the selectivity. One advantage of the compositional change is that the enantiomers of molecules **A**, **D**, **X**, **Y** and **Z** can now be separated with the chiral surface. Furthermore, this separation can be induced by either decreasing or increasing the energy of adsorption of the additional segment on the active site. In the latter case, we can observe that the selectivity becomes smaller than one when the adsorption energy of the additional segment exceeds 2.0. This interesting effect means that the selectivity of the surface reverses when the

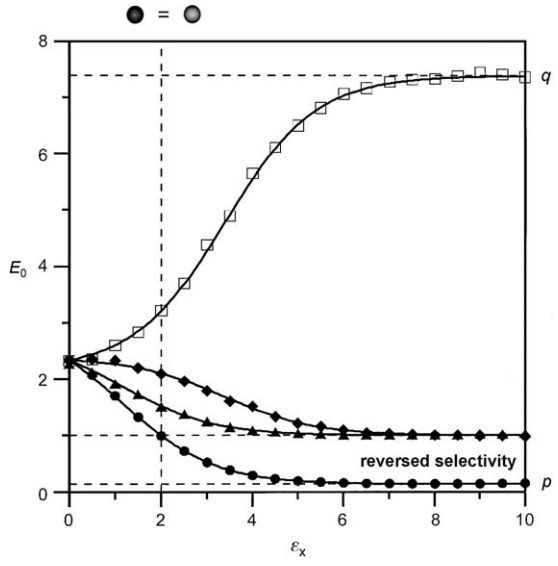

Figure 6. Influence of the composition of the molecules from Figure 2 on the selectivity at the zero-pressure limit. The symbols are the results of the MC simulations whereas the lines are the predictions of the theory. The curves plotted in the figure demonstrate how the energy of adsorption of the additional segment on the active site (ε_x) affects the selectivity: □: **C**; ◆ **E**, **F**; ▲ **B**; ● **A**, **D**, **X**, **Y**, **Z**. These results were obtained for the segment-active site adsorption energy, ε_a equal to 2. The dashed vertical line corresponds to the homogeneous composition of the molecules ($\varepsilon_{x=}\varepsilon_a$). The dashed horizontal lines marked by p and q are the lower and upper selectivity limits for the set of molecules **A**–**Z**, respectively.

additional segments of molecules **A**, **D**, **X**, **Y** and **Z** interact strongly with the active sites. In this case, an effective separation of the enantiomers is still possible, but the preferred enantiomer is *R*.

Note also that making molecule **C** heterogeneous by increasing the adsorption energy of the additional segment beyond 2.0 results in a substantial growth of the selectivity. On the other hand, when interaction of the additional segment with the active site is weaker relative to the remaining part of molecule **C** the selectivity drops sharply. The opposite effect can be observed for all of the remaining molecules. Namely, for molecules **A**, **B**, **D**, **E**, **F**, **X**, **Y** and **Z** the selectivity is a monotonically decreasing function of the adsorption energy of the additional segment. In consequence, the selectivity for these molecules grows when the adsorption energy of the additional segment decreases below 2.0. Moreover, the curves plotted for molecules **E** and **F** overlap. The same refers also to the curves obtained for molecules **A**, **D**, **X**, **Y** and **Z**, that is, to molecules for which the homogeneous enantiomers cannot be separated with the chiral surface. Note, however, that there is one substantial difference between the two groups of the overlaid curves mentioned above. Specifically, in the case of molecules **E**, **F** and also **B,** the selectivity tends to one as the adsorption energy becomes sufficiently high, reflecting a complete loss of the enantiospecific properties of the surface.

Another important feature of the curves from Figure 6 is that they have a common starting point. This point corresponds to the original Γ-shaped molecule with the additional segment being totally inert. Because we are dealing with a very low density of the adsorbed phase, the position of the additional segment within the molecule is irrelevant to the selectivity at the zero-pressure limit. The adsorbed molecules have enough room not to exclude each other such that the presence of the additional inert segment does not affect the separation. In other words in this coverage regime each of the molecules **A**–**Z** adsorbs as if it was molecule **Γ**, which results in the same selectivity equal to 2.33. Regarding the endpoints of the curves shown in Figure 6, we can observe that there are two limiting values p and q that span the selectivity interval. The first value corresponds exclusively to molecule **C,** whereas the latter is common for molecules **A**, **D**, **X**, **Y** and **Z**.

To quantify the effect of the energy of adsorption of the additional segment we used the same theoretical method as for the homogeneous molecules. Table 2 shows the selectivity at the zero-pressure limit predicted for the molecules from Figure 2. The second column of the table shows the resulting expressions used for the calculation of the curves from Figure 6 (——). In the third column we listed the limiting forms of the expressions from the second column obtained for an infinitely large energy of adsorption of the additional segment on the active site. The last column of Table 2 gives numerical values of the limiting forms calculated for $\varepsilon_a = 2.0$ and $\varepsilon_b = 0.0$, that is, for the energy parameters corresponding to the results shown in Figure 6. As shown in Figure 6, the theoretical results of Table 2 agree perfectly with the simulations, regardless of the assumed footprint shape. One important piece of information from this table that is not directly obtainable from Figure 6 is the mutual relation between the upper and lower limit of selectivity, p and q. Specifically, from the third column of the table it follows that these quantities are reciprocal and, moreover, they are simple functions of the energy of adsorption of the core segment on the active site. In consequence, the selectivity at the zero-pressure limit, that corresponds to molecule **C** would be equal to the selectivity calculated for molecules **A**, **D**, **X**, **Y** and **Z** adsorbed on the mirror image of our surface. A somewhat paradoxical consequence of this fact is that to remove the *S* enantiomer of **A**, **D**, **X**, **Y** or **Z** from the corresponding racemate, it is necessary to expose the *R*-selective surface to the bulk racemic mixture.

Table 2. Selectivity at the zero-pressure limit, E_o, obtained from the theory for the chiral molecules containing one heterogeneous segment.

Molecule	E_o [a]	E_o^{∞} [b]	$E_o^{\infty}(\varepsilon_a=2.0)$
A, **D**, **X**, **Y**, **Z**	$(z+\alpha)/(z-\beta)$	$\exp(-\varepsilon_a)$	0.13 p
B	$(z+\alpha-\beta)$	1	1.00
C	$(z+\alpha-\beta)/z$	$\exp(\varepsilon_a)$	7.39 q
E, **F**	$(z+\alpha)/z$	1	1.00

[a] $\alpha=\exp(\varepsilon_a)-1$, $\beta=1-\exp(\varepsilon_x)$, $z=4+(5-\beta)/\alpha$. [b] $\varepsilon_x\to\infty$.

To illustrate better the reversal of selectivity observed for molecules **A**, **D**, **X**, **Y** and **Z** in Figure 7, we plotted the isotherms of adsorption of the enantiomers of molecule **A** on the *S*-selective surface. The results in this figure were obtained by assuming a different energy of adsorption of the additional segment on the active site. Specifically, in the first case, we assumed $\varepsilon_a = 2.0 < \varepsilon_x = 3.0$, which represents stron-

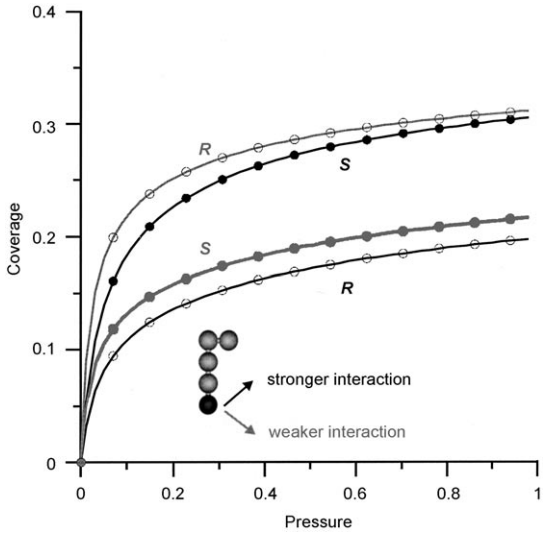

Figure 7. Partial isotherms of adsorption of the enantiomers of molecule **A** on the *S*-selective surface. The results plotted in the figure correspond to two different values of the energy of interaction between the additional segment and the active site, ε_x. The simulations were performed for ε_a equal to 2, and for ε_x equal to 1 (weaker interaction) and 3 (stronger interaction). Pressure is given in arbitrary units.

ger adsorption of the additional segment on the active site. In the second case, we assumed $\varepsilon_a = 2.0 > \varepsilon_x = 1.0$ corresponding to a weak interaction between the additional segment and the active site. As clearly follows from Figure 7, the above changes result in completely different relative positions of the partial isotherms for the *R* and *S* enantiomers. For the decreased adsorption energy of the additional segment the sequence of the partial isotherms is identical to that observed for the original Γ-shaped molecule (see Figure 1). In this case, the enantiomer *S* is preferentially adsorbed from the mixture. On the contrary, when the adsorption energy of the additional segment is larger than ε_a the sequence of the partial isotherms reverses.

The results of this section show that an increased adsorption energy for the additional segment is, in general, beneficial for the separation of the enantiomers of molecules **A**, **C**, **D**, **X**, **Y** and **Z**. In the case of molecule **C,** the modification results in a highly preferential adsorption of the *S* enantiomer on the *S*-selective surface. On the other hand, for molecules **A**, **D**, **X**, **Y** and **Z** the effectiveness of the separation can be as high as that seen for molecule **C**, but now the preferred enantiomer is *R*. For these five molecules it is also possible to increase the selectivity by decreasing the energy of adsorption of the additional segment on the active site down to zero. However, this procedure gives a selectivity that cannot be higher than the selectivity obtained for the original Γ-shaped molecule.

Conclusion

Our observations demonstrate that the model nanostructured surface provides an effective mechanism for chiral selection, which can be an alternative to those inherent in conventional chiral adsorbents, such as CSPs and chirally templated surfaces. The results of this work give useful insights into the interplay between the structure of the surface and the geometry of the adsorbate. They hint at how to correlate these two factors to improve the separation of chiral molecules with nanoarrays of active centres. The main advantage of the proposed chiral adsorbent is the great possibility for tuning the selectivity by changing the interaction pattern of the enantiomers with the surface. As we demonstrated, in some instances subtle differences in the interaction pattern can lead to a reversal of the selectivity. Moreover, the extent of the separation on the chiral surface can be tuned by manipulating the footprint of the adsorbing molecules. This can be done for example by derivatisation of one chiral molecule to obtain another molecule with the footprint shape resulting in the highest enantioselectivity. Our theoretical approach provides strategies that enable prediction of this footprint. In particular, the theory allows for the calculation of the selectivity at low pressures, a property which is especially important for analytical chromatography or chiral catalysis. The proposed model implies the potential to construct chiral nanostructures with programmable functionalities by the appropriate choice of the active and inert sites.

Acknowledgements

This work was supported by the Polish Ministry of Science and Higher Education (grant no. 1 T09A 103 30). The author thanks D.S. Sholl for helpful discussions.

[1] S. C. Stinson, *Chem. Eng. News* **2001**, *79*(20), 45–57.
[2] N. M. Maier, P. Franco, W. J. Lindner, *J. Chromatogr. A* **2001**, *906*, 3–33.
[3] S. Ahuja, *Chiral Separations by Chromatography*, Oxford University Press, Washington, **2000**.
[4] W. H. Pirkle, T. C. Pochapsky, *Chem. Rev.* **1989**, *89*, 347–362.
[5] T. Fornstedt, P. Sajonz, G. Guiochon, *J. Am. Chem. Soc.* **1997**, *119*, 1254–1264.
[6] A. Cavazzini, K. Kaczmarski, P. Szabelski, D. Zhou, X. Liu, G. Guiochon, *Anal. Chem.* **2001**, *73*, 5704–5715.
[7] T. Fornstedt, G. Zhong, Z. Bensetiti, G. Guiochon, *Anal. Chem.* **1996**, *68*, 2370–2378.
[8] T. Fornstedt, G. Götmar, M. Andersson, G. Guiochon, *J. Am. Chem. Soc.* **1999**, *121*, 1164–1174.
[9] G. Götmar, T. Fornstedt, M. Andersson, G. Guiochon, *J. Chromatogr. A* **2001**, *905*, 3–17.
[10] Q. Fu, H. Sanbe, C. Kagawa, KK. Kunimoto, J. Haginaka, *Anal. Chem.* **2003**, *75*, 191–198.
[11] G. Götmar, R. N. Alberada, T. Fornstedt, *Anal. Chem.* **2002**, *74*, 2950–2959.
[12] D. Rampulla, A. J. Gellman in *Dekker Encyclopedia of Nanoscience and Nanotechnology* (Eds.: J. A. Schwarz, C. I. Contescu, K. Putyera), Marcel Dekker, New York, **2004**, pp. 1113–1123.
[13] V. Humbolt, S. M. Barlow, R. Raval, *Prog. Surf. Sci.* **2004**, *76*, 1–19.
[14] K. H. Ernst, *Curr. Opin. Colloid Interface Sci.* **2008**, *13*, 54–59.
[15] Q. Chen, N. V. Richardson, *Annu. Rep. Prog. Chem., Sect. C* **2004**, *100*, 313–347.
[16] L. Pérez-García, D. B. Amabilino, *Chem. Soc. Rev.* **2007**, *36*, 941–967.
[17] L. Pérez-García, D. B. Amabilino, *Chem. Soc. Rev.* **2002**, *31*, 342–356.
[18] K. H. Ernst, *Top. Curr. Chem.* **2006**, *265*, 209–252.
[19] C. F. McFadden, P. S. Cremer, A. J. Gellman, *Langmuir* **1996**, *12*, 2483–2487.
[20] J. D. Horvath, and A. J. Gellman, *J. Am. Chem. Soc.* **2002**, *124*, 2384–2392.
[21] J. D. Horvath, and A. J. Gellman, *J. Am. Chem. Soc.* **2001**, *123*, 7953–7954.
[22] T. Greber, Ž. Šljivančanin, R. Schillinger, J. Wider, B. Hammer, *Phys. Rev. Lett.* **2006**, *96*, 056103.
[23] J. D. Horvath, A. Koritnik, P. Kamakoti, D. S. Sholl, A. J. Gellman, *J. Am. Chem. Soc.* **2004**, *126*, 14988–14994.
[24] A. Ahmadi, G. Attard, J. Feliu, A. Rodes, *Langmuir* **1999**, *15*, 2420–2424.
[25] D. Stacchiola, L. Burkholder, W. T. Tysoe, *J. Am. Chem. Soc.* **2002**, *124*, 8984–8989.
[26] I. Lee, F. Zaera, *J. Am. Chem. Soc.* **2006**, *128*, 8890–8898.
[27] D. Stacchiola, L. Burkholder, T. Zheng, M. Weinert, W. T. Tysoe, *J. Phys. Chem. B* **2005**, *109*, 851–856.
[28] I. Lee, F. Zaera, *J. Phys. Chem. B* **2005**, *109*, 12920–12926.
[29] M. Ortega-Lorenzo, S. Haq, T. Bertrams, P. Murray, R. Raval, C. J. Baddeley, *J. Phys. Chem. B* **1999**, *103*, 10661–10669.
[30] W. A. Bonner, P. R. Kavasmaneck, F. S. Martin, J. J. Flores, *Science* **1974**, *186*, 143.
[31] R. Hazen, D. S. Sholl, *Nature Mater.* **2003**, *2*, 367–374.
[32] D. S. Sholl, A. Asthagiri, and T. D. Power, *J. Phys. Chem. B* **2001**, *105*, 4771–4782.
[33] D. S. Sholl, *Langmuir* **1998**, *14*, 862–867.
[34] T. D. Power, D. S. Sholl, *J. Vac. Sci. Technol. A* **1999**, *17*, 1700–1704.
[35] R. Raval, *CATTECH* **2001**, *5*, 12–28.
[36] T. Mallat, E. Orglmeister, A. Baiker, *Chem. Rev.* **2007**, *107*, 4863–4890.

[37] J. N. James, D. S. Sholl, *Curr. Opin. Colloid Interface Sci.* **2008**, *13*, 60–64, and references therein.
[38] K. B. Lipkowitz, *Acc. Chem. Res.* **2000**, *33*, 555–562.
[39] K. B. Lipkowitz, *J. Chromatogr. A* **2001**, *906*, 417–442.
[40] S. Schefzick, W. Lindner, K. B. Lipkowitz, M. Jalaie, *Chirality* **2000**, *12*, 7–15.
[41] K. B. Lipkowitz, R. Coner, M. A. Peterson, *J. Am. Chem. Soc.* **1997**, *119*, 11269–11276.
[42] E. Alvira, J. I. García, J. A. Mayoral, *Chem. Phys.* **1999**, *240*, 101–108.
[43] Y. H. Choi, C. H. Yang, H. W. Kim, S. Jung, *Carbohydr. Res.* **2000**, *328*, 393–397.
[44] F. Roma, G. Zgrablich, D. Stacchiola, W. T. Tysoe, *J. Chem. Phys.* **2003**, *118*, 6030–6037.
[45] F. Roma, D. Stacchiola, W. T. Tysoe, G. Zgrablich, *Phys. A* **2004**, *338*, 493–510.
[46] P. Szabelski, J. Talbot, *J. Comput. Chem.* **2004**, *25*, 1779–1786.
[47] P. Szabelski, *Appl. Surf. Sci.* **2004**, *227*, 94–103.
[48] P. Szabelski, *Appl. Surf. Sci.* **2007**, *253*, 5387–5392.
[49] P. Szabelski, D. S. Sholl, *J. Chem. Phys.* **2007**, *126*, 144709.
[50] P. Szabelski, D. S. Sholl, *J. Phys. Chem. C* **2007**, *111*, 11936–11942.
[51] P. Szabelski, *J. Comput. Chem.* **2008**, *29*, 1615–1625.
[52] P. Szabelski, *J. Chem. Phys.* **2008**, *128*, 184702.
[53] H. Xu, K. Y. S. Ng, *Surf. Sci.* **1996**, *356*, 19–27.
[54] M. Saidy, O. L. Warren, P. A. Thiel, K. A. R. Mitchell, *Surf. Sci.* **2001**, *494*, L799–L804.
[55] R. Fasel, M. Gierer, H. Bludau, P. Aebi, J. Osterwalder, and L. Schlapbach, *Surf. Sci.* **1997**, *374*, 104–116.
[56] R. Fasel, P. Aebi, L. Schlapbach, T. Greber, and J. Osterwalder, *Surf. Rev. Lett.* **1997**, *4*, 1155–1160.
[57] H. Spillmann, A. Dmitriev, N. Li, P. Messina, J. V. Barth, K. Kern, *J. Am. Chem. Soc.* **2003**, *125*, 10725–10728.
[58] J. Henzie, J. E. Barton, C. L. Stender, T. W. Odom, *Acc. Chem. Res.* **2007**, *40*, 249–257.
[59] A. J. Ramirez-Pastor, M. S. Nazarro, J. L. Riccardo, G. Zgrablich, *Surf. Sci.* **1995**, *341*, 249–261.
[60] A. J. Ramirez-Pastor, J. L. Riccardo, V. Pereyra, *Langmuir* **2000**, *16*, 682–689.
[61] A. J. Ramirez-Pastor, V. Pereyra, J. L. Riccardo, *Langmuir* **1999**,*15*, 5707–5712.
[62] P. Szabelski, K. Kaczmarski, *J. Chromatogr. A* **2006**, *1113*, 74–83.

Received: March 11, 2008
Published online: July 21, 2008

